Since January 2020 Elsevier has created a COVID-19 resource centre with free information in English and Mandarin on the novel coronavirus COVID-19. The COVID-19 resource centre is hosted on Elsevier Connect, the company's public news and information website.

Infectious Disease Modelling 7 (2022) 795–810

Contents lists available at ScienceDirect

Infectious Disease Modelling

journal homepage: www.keaipublishing.com/idm

Evaluations of COVID-19 epidemic models with multiple susceptible compartments using exponential and non-exponential distribution for disease stages

Yan Chen [a], Haitao Song [b], Shengqiang Liu [a, *]

[a] School of Mathematical Sciences, Tiangong University, Tianjin, 300387, China
[b] Complex Systems Research Center, Shanxi University, Taiyuan, 030006, China

ARTICLE INFO

Article history:
Received 31 August 2022
Received in revised form 7 November 2022
Accepted 8 November 2022
Available online 15 November 2022
Handling Editor: Y. Shao

Keywords:
Mathematical models
COVID-19
Exponential distribution
Gamma distribution
Peak time

ABSTRACT

Mathematical models have wide applications in studying COVID-19 epidemic transmission dynamics, however, most mathematical models do not take into account the heterogeneity of susceptible populations and the non-exponential distribution infectious period. This paper attempts to investigate whether non-exponentially distributed infectious period can better characterize the transmission process in heterogeneous susceptible populations and how it impacts the control strategies. For this purpose, we establish two COVID-19 epidemic models with heterogeneous susceptible populations based on different assumptions for infectious period: the first one is an exponential distribution model (EDM), and the other one is a gamma distribution model (GDM); explicit formula of peak time of the EDM is presented via our analytical approach. By data fitting with the COVID-19 (Omicron) epidemic in Spain and Norway, it seems that Spain is more suitable for EDM while Norway is more suitable for GDM. Finally, we use EDM and GDM to evaluate the impaction of control strategies such as reduction of transmission rates, and increase of primary course rate (PCR) and booster dose rate (BDR).

1. Introduction

Epidemics such as tuberculosis, smallpox, SARS, MERS and Ebola had significantly affected human history. Coronavirus disease (COVID-19) has swept the whole world since 2019. By July 2022, nearly 600 million people worldwide had been infected and more than 6 million people had been killed by COVID-19 (Coronavirus COVID, 2019). Mathematical models have been widely applied to study the transmission dynamics of COVID-19 (Humphrey et al., 2021; Li et al., 2020; Musa et al., 2021; Song et al., 2020, 2021a, 2021b, 2022; Wei et al., 2022). Mathematical models are very helpful in understanding the transmission dynamics of infectious diseases as well as identifying proper strategies for the control and prevention of the epidemic. From the SIR model proposed by Kermack and McKendrick(Kermack & McKendrick, 1927) to the later SEIR model (Greenhalgh, 1992; Kuznetsov & Piccardi, 1994; Li & Muldowney, 1995; Tomchin and Fradkov, 2020) and other more complex

* Corresponding author.
E-mail addresses: y_chen00@163.com (Y. Chen), htsong@sxu.edu.cn (H. Song), sqliu@tiangong.edu.cn (S. Liu).
Peer review under responsibility of KeAi Communications Co., Ltd.

https://doi.org/10.1016/j.idm.2022.11.004

models with hospitalization or isolation compartments (Brauer, 2015), these models can well describe the transmission process of infectious diseases and have produced many applications. For example, it helps people to study the impact of certain control measures, including wearing masks(Kabir et al., 2021), reducing parties (Djaoue et al., 2020), vaccinating (Braud, 2018; Sivadas et al., 1770) and isolating (An et al., 2021) on disease transmission.

During the epidemic of COVID-19, the heterogeneity of susceptible populations may occur due to the difference of individuals in vaccinations, some recent excellent applications have appeared(Liu et al., 2008; Okuonghae, 2013). In addition, most mathematical models assume exponential distribution for the infectious period, however, for many infectious diseases, the distributions for the infectious period may not be exponential(Wearing et al., 2005; Bolzoni et al., 2021; Wang et al., 2017; Krylova and Earn, 2013; Lloyd, 1470; Feng et al., 2007; Feng et al., 2016)–(Wearing et al., 2005; Bolzoni et al., 2021; Wang et al., 2017; Krylova and Earn, 2013; Lloyd, 1470; Feng et al., 2007; Feng et al., 2016). Recently, there have been many excellent literatures supporting non-exponentially distributed infectious period for COVID-19: In (Verity et al., 2019), based on Bayesian methods to fit the infectious period data from 169 COVID-19 cases, Verity et al. found out the infectious period obeys the gamma distribution. Blyuss et al. use an SEIR-type mathematical model with non-exponential distribution of incubation and infectious periods to investigate the dynamics and containment of COVID-19 (Blyuss & Kyrychko, 2021). In (Capistran et al., 2021), Capistran et al. proposed COVID-19 mathematical model with non-exponentially distributed infectious period to predict hospital demand in metropolitan areas during the COVID-19 pandemic and estimate the lockdown-induced 2nd waves. Thus it remains an interesting problem of how the non-exponential distribution for infectious period of mathematical models with heterogeneous susceptible populations affects the COVID-19 epidemic transmission dynamics and control measures. As far as we know, this issue has not been well studied.

In 2007, Feng(Feng, 2007) made profound progress by obtaining an explicit formula on the peak value for the mathematical epidemic model with multiple infected compartments and non-exponentially distributed infectious period. However, Feng's work (Feng, 2007) is only applicable to one susceptible compartment, thus it is worth considering how to extend it to multiple susceptible compartments. On the other hand, peak time is a very important to evaluate the epidemic in understanding the epidemic process so as to reasonably allocate medical resources. However, there are very few literatures even for the most classical SIR model until the recent excellent work by Turkyilmazoglu (Turkyilmazoglu, 2021). In this paper, motivated by the above works of Feng(Feng, 2007) and Turkyilmazoglu(Turkyilmazoglu, 2021), we will investigate whether non-exponentially distributed infectious period can better characterize the COVID-19 transmission process in heterogeneous susceptible populations and how it impacts the control strategies.

The paper is organized as follows. In section 2, based on SIR model, we establish a mathematical model with heterogeneous susceptible populations and general distribution for infectious period. Then, we degenerate the general distribution model into exponential distribution model (EDM) and Gamma distribution model (GDM) and make a detailed theoretical derivation for the peak value, peak time, final size and the basic reproduction number R_0. In section 3, the epidemic data of Spain and Norway are used to fit with EDM and GDM respectively. It is found that the simulation results of EDM are more consistent with the data of Spain while those of GDM are more consistent with the data of Norway. In addition, based on the data from these two countries, we also investigate the effectiveness of different control measures on GDM and EDM. The results show that they are consistent, but GDM tends to predict higher peak value and lower peak time. Section 4 includes some concluding remarks and discussions.

2. Model and analysis

2.1. The basic model

The models in this paper are extensions of the standard SIR model (without vital dynamics):

$$\begin{cases} \dot{S} = -\beta SI, \\ \dot{I} = \beta SI - \gamma I, \\ \dot{R} = \gamma I. \end{cases} \tag{1}$$

The initial conditions of the system are: $S(0) = S_0$, $I(0) = I_0$ and $R(0) = R_0$. Here, $S(t)$, $I(t)$, and $R(t)$ represent the number of susceptible, infectious, and recovered individuals at time t. At the same time, $S(t) + I(t) + R(t) = N$. N is the total number of people in the system, β is transmission coefficient, γ is the recover rate.

The SIR model implicitly assumes that the infectious period is exponentially distributed with $1/\gamma$ being the mean value of the infectious period. Although it is an option to assume that the infectious period is exponential distribution (see Fig. 1), it is also an attempt to assume that the infectious period is other distribution. In previous studies, it is found that the infectious

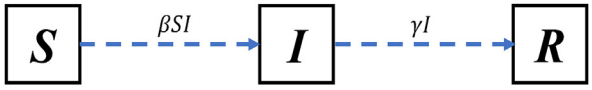

Fig. 1. The classic SIR model.

stage of many infectious diseases may be closer to the gamma distribution(Feng et al., 2007; Wearing et al., 2005). Considering that vaccines have become a very important measure for us to deal with infectious diseases, in order to make the model more realistic, we divide the susceptible population into two types. One is vaccinated (S_v) and the other is not vaccinated (S_n). An extended SIR model is obtained with death compartment.

2.2. The model with a general distribution of infectious period

In 2016, Feng et al. established a general distribution model using the method of probability(Feng et al., 2016). Referring to the research method, we establish the model described in Fig. 2: S_n and S_v inflow I class is given by

$$\dot{S_n} = -\beta S_n I, \tag{2}$$

$$\dot{S_v} = -\epsilon\beta S_v I. \tag{3}$$

Let $S = S_n + S_v$, then $\dot{S} = -I\lambda(t)$, where $\lambda(t)$ denotes the force of infection given by

$$\lambda(t) = \beta(\epsilon S_v + S_n). \tag{4}$$

Total number of infected individuals at time t, $I(t)$ is given by

$$I(t) = \int_0^t \lambda(s) I M(t-s) ds + I(0) M(t). \tag{5}$$

The first term in (5) represents the number of individuals who remain infectious after $t - s$ time units since onset at time s $(0 < s < t)$. The second term in (5) represents the number of individuals infected at time 0 and still in I class at time t. Let $g_M = -\dot{M}(s)$ represent the probability density function of $M(s)$. Meanwhile, g_M gives the rate of leaving I class. For more detailed explanation, see Feng et al. (Feng et al., 2007) and Feng and Thieme(Feng & Thieme, 2000). Differentiating $I(t)$:

$$\dot{I}(t) = \lambda(t) I - \left[\int_0^t \lambda(s) I g_M(t-s) ds + I(0) g_M(t) \right]. \tag{6}$$

In (6), the first term is individuals from the susceptible S to I classes, the second term is the infectious individuals leaving I class. The total number of deaths at time t is:

$$D(t) = \int_0^t p \left[\int_0^\tau \lambda(s) I g_M(\tau - s) ds + I(0) g_M(\tau) \right] d\tau. \tag{7}$$

In brackets of (7), the former item denotes that the individuals are infected at time s and leave the I class at time τ, and the latter item denotes that the individuals are infected at the initial moment and leave the I class at time τ. p is the infection fatality rate (the proportion of individuals entering D class after leaving I class). Differentiating $D(t)$:

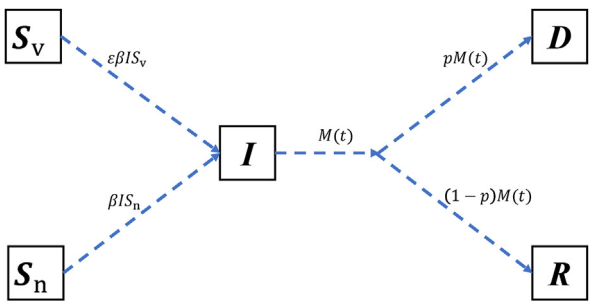

Fig. 2. Extended SIR model transmission and progression flows.

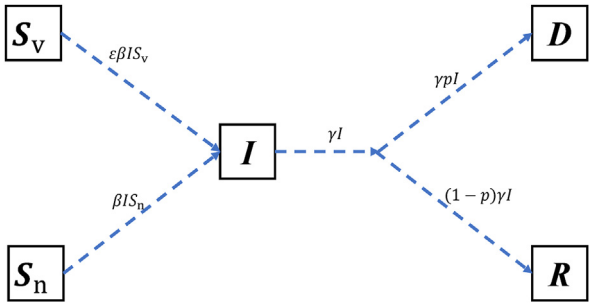

Fig. 3. Epidemic process of EDM.

$$\dot{D}(t) = p\left[\int_0^t \lambda(s) I g_M(t-s)ds + I(0)g_M(t)\right]. \tag{8}$$

Similarly, the total number of recovered individuals at time t is:

$$R(t) = \int_0^t (1-p)\left[\int_0^\tau \lambda(s) I g_M(\tau - s)ds + I(0)g_M(\tau)\right]d\tau. \tag{9}$$

The explanation of $R(t)$ is similar to $D(t)$. Differentiating $R(t)$:

$$\dot{R}(t) = (1-p)\left[\int_0^t \lambda(s) I g_M(t-s)ds + I(0)g_M(t)\right]. \tag{10}$$

With the above equation, we obtain the system of integral and differential equations for the general distribution model,

$$\begin{cases} \dot{S_n} = -\beta S_n I, \\ \dot{S_v} = -\epsilon\beta S_v I, \\ \dot{I}(t) = \lambda(t)I - \left[\int_0^t \lambda(s) I g_M(t-s)ds + I(0)g_M(t)\right], \\ \dot{D}(t) = p\left[\int_0^t \lambda(s) I g_M(t-s)ds + I(0)g_M(t)\right], \\ \dot{R}(t) = (1-p)\left[\int_0^t \lambda(s) I g_M(t-s)ds + I(0)g_M(t)\right]. \end{cases} \tag{11}$$

where $\lambda(t)$ is given in (4). The initial condition is $(S_v(0), S_n(0), I(0), D(0), R(0)) = (S_{v0}, S_{n0}, I_0, D_0, R_0)$. We note that the infectious period in the system (11) is general distribution. Next, we use exponential distribution and gamma distribution instead of general distribution to obtain two ODE models with different distributions.

2.3. Exponential distribution model(EDM): explicit formula for peak time

Let $M(t) = e^{-\gamma t}$, then $g_M(t) = \gamma e^{-\gamma t}$, thus system (11)'s digram can be simplified as Fig. 3, and the model could be shown as follows:

$$\begin{cases} \dot{S}_n = -\beta S_n I, & (12)\\ \dot{S}_v = -\varepsilon\beta S_v I, & (13)\\ \dot{I}(t) = \beta(\varepsilon S_v + S_n)I - \gamma I, & (14)\\ \dot{D}(t) = p\gamma I, & (15)\\ \dot{R}(t) = (1-p)\gamma I. & (16) \end{cases}$$

Motivated to the method in 2021 (Turkyilmazoglu, 2021) on the derivation of the explicit formula for peak time of the classic Kermack-McKendrick SIR model, now we will develop the techniques in (Turkyilmazoglu, 2021) and construct the explicit formula for peak time and peak value of the above system.

From (12) and (13), $\frac{dS_v}{dS_n} = \epsilon\frac{S_v}{S_n}$, from which we are able to get:

$$S_v(t) = \frac{S_n^\epsilon(t)}{S_{n0}^\epsilon} S_{v0}. \tag{17}$$

Since $\dot{S}_v$ and $\dot{S}_n < 0$ all $t > 0$, then S_v and S_n must obtain their maximum values at the initial moment. We observe (14) and find that $\dot{I} > 0$ if and only if $\beta(\epsilon S_v + S_n) - \gamma > 0$. Therefore, there are only two cases of $\dot{I}$: one is positive first and then negative, and the maximum value is obtained when $\dot{I}$ changes sign. The other is always negative, which cannot constitute an epidemic, so we neglect this case. Let's just focus on the first case. From (14) and (17), we get

$$\dot{I}(t) = \beta\left(\epsilon\frac{S_n^\epsilon}{S_{n0}^\epsilon} S_{v0} + S_n\right) I - \gamma I. \tag{18}$$

Let the right hand of (18) equal to 0, we get

$$\beta\left(\epsilon\frac{S_n^\epsilon(t)}{S_{n0}^\epsilon} S_{v0} + S_n\right) = \gamma. \tag{19}$$

The above equation (19) is a monadic equation on S_n, thus by solving this equation, there exists a unique implicit solution for S_n, denoted as S_n^*. Therefore, $I(t)$ reaches its peak value as $S_n(t) = S_n^*$ holds true.

From (12) and (18), we get $\frac{dI}{dS_n} = -\epsilon\frac{S_{v0}}{S_{n0}^\epsilon} S_n^{\epsilon-1} - 1 + \frac{\gamma}{\beta S_n}$. Integrating t from 0 to t, then we have:

$$I(t) = S_{v0} + S_{n0} - \frac{S_{v0}}{S_{n0}^\epsilon} S_n^\epsilon - S_n + \frac{\gamma}{\beta}\ln\frac{S_n}{S_{n0}} + I_0 \triangleq f(S_n). \tag{20}$$

Thus from (20) we obtain the peak value of $I(t)$ when $S_n = S_n^*$, that is

$$I_{max} = S_{v0} + S_{n0} - \frac{S_{v0}}{S_{n0}^\epsilon} S_n^{*\epsilon} - S_n^* + \frac{\gamma}{\beta}\ln\frac{S_n^*}{S_{n0}} + I_0.$$

From (12) we get: $\frac{dt}{dS_n} = \frac{1}{-\beta S_n I}$. Integrating t over 0 to t, we have:

$$t = -\int_{S_{n0}}^{S_n(t)} \frac{1}{\beta S_n f(S_n)} dS_n. \tag{21}$$

Noting that $S_n = S_n^*$ corresponds to the peak time of the infectious, hence from (21) we obtain the following explicitly formula for peak time, where $f(S_n)$ was defined in (20):

$$t_{max} = \int_{S_{n0}}^{S_n^*} \frac{1}{-\beta S_n f(S_n)} dS_n.$$

By the next generation matrix method calculate basic reproductive number $\Re_0$ (van den Driessche et al., 2008)

$$\Re_0 = \frac{\beta(\epsilon S_{v0} + S_{n0})}{\gamma}. \tag{22}$$

Final size Z is a quantitative value which reflects the impact of the epidemic(Arino et al., 2007), and is defined as $Z = S(0) - S(\infty)$. From (12)–(14) we get $\frac{d(S+I)}{dt} = -\gamma I$. Thus $S + I$ is decreasing whenever $I > 0$. Since $S + I$ is lower bounded by 0, it has a limit. Hence,

$$\lim_{t\to\infty} \frac{d(S+I)}{dt} = 0,$$

so, $I(\infty) = 0$ (Ma & Earn, 2006). For (20) when $t \to \infty$ we get

$$0 = S_{v0} + S_{n0} - \frac{S_{v0}}{S^{\epsilon}_{n0}} S^{\epsilon}_n(\infty) - S_n(\infty) + \frac{\gamma}{\beta} \ln \frac{S_n(\infty)}{S_{n0}} + I_0.$$

The equation is a monadic equation on $S_n(\infty)$, and solve to get $S_n(\infty)$. Therefore, final size Z

$$\begin{aligned} Z &= S(0) - S(\infty) \\ &= S_{v0} + S_{n0} - S_v(\infty) - S_n(\infty) \\ &= S_{v0} + S_{n0} - \frac{S_{v0}}{S^{\epsilon}_{n0}} S^{\epsilon}_n(\infty) - S_n(\infty). \end{aligned}$$

2.4. Gamma distribution model(GDM)

Let $M(t) = \sum_{j=1}^{n} \frac{(n\gamma_1 t)^{j-1} e^{-n\gamma_1 t}}{(j-1)!}$, then $g_M(t) = \frac{n\gamma_1 (n\gamma_1 t)^{n-1}}{(n-1)!} e^{-n\gamma_1 t}$. Thus using on the similar arguments for the GDM in (Feng et al., 2007, 2016), system (11) can be simplified to:

$$\begin{cases} \dot{S}_n = -\beta S_n I, & (23) \\ \dot{S}_v = -\varepsilon\beta S_v I, & (24) \\ \dot{I}_1(t) = \beta(\varepsilon S_v + S_n) I - n\gamma_1 I_1, & (25) \\ \dot{I}_j(t) = n\gamma_1 I_{j-1} - n\gamma_1 I_j, \quad for\, j = 2..n & (26) \\ \dot{D}(t) = pn\gamma_1 I_n, & (27) \\ \dot{R}(t) = (1-p) n\gamma_1 I_n, & (28) \\ \text{with} \quad I = \sum_{j=1}^{n} I_j. \end{cases}$$

Previous studies have so far not given analytical solutions for peak value and time of infectious disease models with multiple infectious compartments. Since the infectious disease models with gamma distribution for infectious period is similar to infectious disease models with multiple infectious compartments, it is difficult to find the analytical solution of peak value and time.

Fortunately, Feng et al., in 2007 proposed a new peak value(Feng, 2007), which can be solved analytically for infectious disease models with multiple infectious compartments. Next, we try to extend the peak value to infectious disease models with multiple susceptible compartments. Consider the system:

$$\begin{cases} \dot{S}_1 = -\beta b x a_1 S_1, \\ \dot{S}_j = -\beta b x a_j S_j, \quad for\, j = 2 \ldots n \\ \dot{x} = \Pi \beta b x a S - V x, \\ \dot{R} = w x. \end{cases} \tag{29}$$

Here, $a = (a_1, a_2, \ldots, a_n)^{\mathrm{T}}$ is a row vector with the components representing the rate at which different susceptible compartments are infected (reflecting different immunity); $y = (S_1, S_2, \ldots, S_n)$ is a column vector whose components are different susceptible compartments; $S = \sum_{j=1}^{n} S_j$ is the total number of susceptible populations. Other the notations are adopted from (Feng, 2007). In the system (29), we get the force of infection $\Lambda(x) = \beta b x$ and the reproductive number $\mathcal{R} = \beta b V^{-1} \Pi$. A new peak value is defined as,

$$Y = \frac{1}{\mathcal{R}} \beta b V^{-1} x,$$

then Y satisfies the following differential equation,

$$\dot{Y} = \Lambda(x)\left(ay - \frac{1}{\mathcal{R}}\right).$$

In GDM system, the transmission ability is equal for $I_j (j = 1 \ldots n)$, then we have $b = (1, 1, \ldots, 1) \in R^n$, $a = (1,\epsilon)^{\mathrm{T}} \in R^2$, $y = (S_n, S_v) \in R^2$,

$$x = \begin{pmatrix} I_1 \\ I_2 \\ \vdots \\ I_{n-1} \\ I_n \end{pmatrix}, \Pi = \begin{pmatrix} 1 \\ 0 \\ 0 \\ \vdots \\ 0 \end{pmatrix}, V = \begin{pmatrix} n\gamma_1 & 0 & \cdots & 0 & 0 \\ -n\gamma_1 & n\gamma_1 & 0 & \ddots & 0 \\ 0 & -n\gamma_1 & \ddots & 0 & 0 \\ \vdots & \ddots & -n\gamma_1 & n\gamma_1 & 0 \\ 0 & \cdots & 0 & -n\gamma_1 & n\gamma_1 \end{pmatrix}_{n\times n}.$$

Here, the force of infection is $\Lambda(x) = \beta\sum_{j=1}^{n} I_j = \beta I$ and the reproductive number is $\mathcal{R} = \frac{\beta}{\gamma_1}$, and then the peak value is

$$Y(t) = \sum_{j=1}^{n} c_j I_j, \quad \text{where} \quad c_j = \frac{n+1-j}{n}.$$

$$\dot{Y}(t) = \beta I\left(\epsilon S_v + S_n - \frac{1}{\mathcal{R}}\right). \tag{30}$$

Similar to $I(t)$ in EDM, when $\dot{Y} = 0$, the maximum value of $Y(t)$ is obtained.

From (17) and (30), we get the value of S_n satisfying $\dot{Y} = 0$, written as $\tilde{S_n}$. From (17), (23) and (30), Y and S_n satisfy the equation

$$\frac{\mathrm{d}Y}{\mathrm{d}S_n} = -\epsilon\frac{S_{v0}}{S_{n0}^{\epsilon}}S_n^{\epsilon-1} - 1 + \frac{\gamma_1}{\beta S_n}.$$

Integrating over 0 to t:

$$Y(t) = S_{v0} + S_{n0} - \frac{S_{v0}}{S_{n0}^{\epsilon}}S_n^{\epsilon} - S_n + \frac{\gamma_1}{\beta}\ln\frac{S_n}{S_{n0}} + Y_0, \tag{31}$$

when $S_n = \tilde{S_n}$, we get peak value $Y_{\max}$

$$Y_{max} = S_{v0} + S_{n0} - \frac{S_{v0}}{S_{n0}^{\epsilon}}\tilde{S_n}^{\epsilon} - \tilde{S_n} + \frac{\gamma_1}{\beta}\ln\frac{\tilde{S_n}}{S_{n0}} + Y_0.$$

However, for the peak time, we cannot give the analytic formula using the previous method because of the difference between the defined $Y(t)$ and $I(t)$. It can only be numerically solved.

By the next generation matrix method, we can get basic reproductive number $\Re_0$ (van den Driessche et al., 2008)

$$\Re_0 = \frac{\beta(\epsilon S_{v0} + S_{n0})}{\gamma_1}. \tag{32}$$

For final size, $Y(\infty) = 0$. For (31) when $t \to \infty$ we get

$$0 = S_{v0} + S_{n0} - \frac{S_{v0}}{S_{n0}^{\epsilon}}S_n^{\epsilon}(\infty) - S_n(\infty) + \frac{\gamma_1}{\beta}\ln\frac{S_n(\infty)}{S_{n0}} + Y_0.$$

The equation is a monadic equation on $S_n(\infty)$, and solve to get $S_n(\infty)$. Therefore, final size Z

$$\begin{aligned} Z &= S(0) - S(\infty) \\ &= S_{v0} + S_{n0} - S_v(\infty) - S_n(\infty) \\ &= S_{v0} + S_{n0} - \frac{S_{v0}}{S_{n0}^{\epsilon}}S_n^{\epsilon}(\infty) - S_n(\infty). \end{aligned}$$

3. Comparison of EDM and GDM based on actual data

In this section, we apply EDM and GDM ($n = 2,3$) to the COVID-19 (Omicron) epidemics in Spain and Norway to investigate the differences between EDM and GDM in describing disease transmission and evaluating control strategies (see Fig. 4).

3.1. Data

In December of 2021, COVID-19 (Omicron) epidemic surged in Europe. We acquire the real data for Spain from December 23, 2021 to March 4, 2022 and Norway from January 8 to March 29, 2022 from Worldometer(Norway COVID, 2022; Spain COVID, 2022). The histograms of daily active infectious individuals and cumulative deaths are shown in Fig. 5.

3.2. Parameter estimation

Previous studies in the transmission of COVID-19 (Omicron) have given the information for most of parameter values.

3.2.1. Infectious period

The average length of infected individuals from infectious till recovery is 6.5 day(Yuan et al., 2022).

3.2.2. Infection fatality rate (IFR)

Research findings and statistics show a strong relationship between IFR and the percentage of the elderly population(-Starke et al., 2020; COVID-19 Weekly Cases and Deaths, 2022). In order to be able to effectively estimate the IFR in Spain (18.49% of seniors over 65 years old(Spain Age structure, 2022)) and Norway (17.43% of seniors over 65 years old (Norway Age structure, 2022)), we use the IFR in Ontario, Canada (18.1% of seniors over 65 years old (Ontario population projections, 2022)) which has a similar proportion of elderly people as Spain and Norway, thus IFR = 0.03% (Ulloa et al., 2022) (see Table 1).

3.2.3. Vaccine effectiveness

Vaccine effectiveness can be calculated from the weighted average of vaccination proportion and effectiveness. Assume that uptake of one dose is completely ineffective, the effectiveness of uptake of primary course is 35.5%, and the effectiveness of uptake one booster dose is 71.4%(Andrews et al., 2021). European Centre for Disease Prevention and Control provides the primary course rate (PCR) and booster dose rate (BDR) during the outbreak in Spain and Norway(COVID-19 Vaccine Tracker | European, 2022), see Tables 2 and 3.

Vaccine effectiveness in Spain:

$$\begin{aligned} VE_{spain} &= \frac{PCR - BDR}{PCR} * 35.5\% + \frac{BDR}{PCR} * 71.4\% \\ &= 55.6\%. \end{aligned} \tag{33}$$

Vaccine effectiveness in Norway:

$$\begin{aligned} VE_{norway} &= \frac{PCR - BDR}{PCR} * 35.5\% + \frac{BDR}{PCR} * 71.4\% \\ &= 60\%. \end{aligned} \tag{34}$$

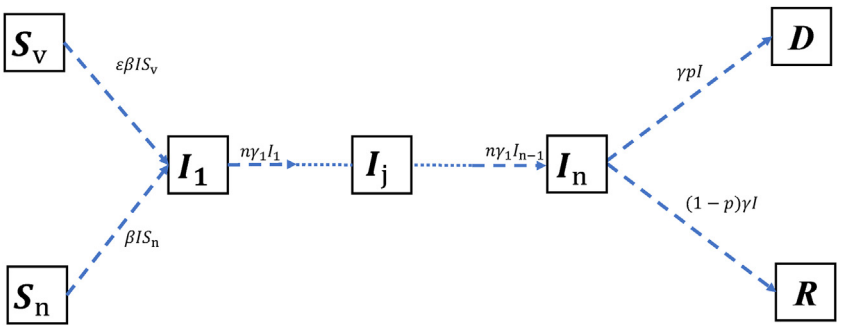

Fig. 4. Epidemic process of EDM.

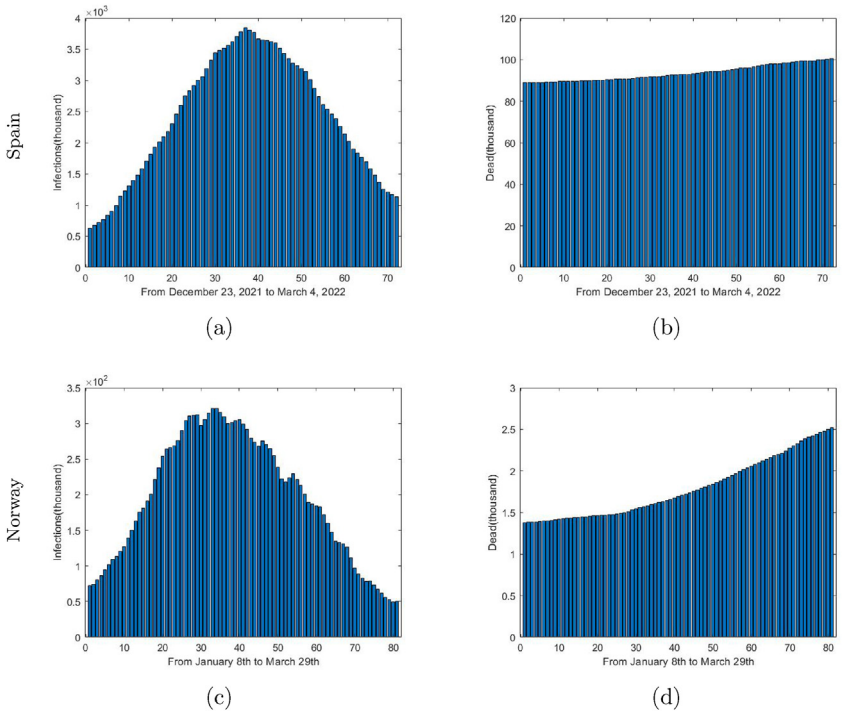

Fig. 5. (a) and (b) show the daily active infectious individuals and cumulative deaths in Spain from December 23, 2021 to March 4, 2022. (c) and (d) show the daily active infectious individuals and cumulative deaths in Norway from January 8 to March 29, 2022.

3.2.4. Initial values

First, we get that the total population of Spain is around $4.6*10^7$ (Spain Population, 2022) and the total population of Norway is around $5.51*10^6$ (Norway Population, 2022). S_{v0} and S_{n0}, the initial value of S_v and S_n, can be calculated by (35) and (36). I_0 and D_0, the initial value of I and D, can be obtained from Fig. 5.

$$\begin{cases} S_{v0} = PCR * (N - I_0 - D_0), & (35) \\ S_{n0} = N - S_{v0} - I_0 - D_0. & (36) \end{cases}$$

What we need to estimate is the transmission coefficients β. Through the least square method, we fit the first 15 days of data in Fig. 5 and each of the three models (EDM, GDM with $n = 2$, GDM with $n = 3$). The results of the fit are shown in Fig. 6 and Tables 4 and 5.

3.3. Analysis of results

Define the average relative error from day 1 to day n as

$$Error = \frac{1}{2n}\sum_{i=1}^{n}\left(\left|\frac{\hat{I}_i - I_i}{I_i}\right| + \left|\frac{\hat{D}_i - D_i}{D_i}\right|\right), \quad (37)$$

where $\hat{I}_i$ and $\hat{D}_i$ denote the number of active infections per day and cumulative deaths predicted by the model, I_i and D_i denote the number of active infections per day and cumulative deaths in the real data.

The comparison of final size, peak value and other parameters with the real data is shown in Tables 6 and 7. The final size from the statistics is much lower than that from the model results, so we speculate that the statistics may have been underestimated due to the excess of asymptomatic. It is easy to find that for Spain, the EDM better describes the COVID-19 (Omicron) transmission process than the GDM, in contrast, for Norway, the GDM is more consistent with the actual data. Also, the same conclusion is shown in Fig. 6. Thus, we speculate that the same infectious disease has different distribution for the infectious period in different countries or regions (may be due to medical conditions, age structure, physical condition of susceptible groups, climate temperature, etc.). Therefore, the distribution for the infectious period must be more cautiously examined, when we use mathematical models to describe the transmission process of infectious diseases.

Table 1
Explanation of symbols.

Symbol	Description
$M(t)$	Probability that an individual remains infectious for t time units since being infected
$\lambda(t)$	Force of susceptibility at time t
$\Lambda(x)$	Force of infection
$1-\epsilon$	Vaccine effectiveness
$1/\gamma$	Mean infectious period with exponential distribution
$1/\gamma_1$	Mean infectious period with Gamma distribution
B	Transmission coefficient
P	Infection fatality rate
N	Total number of people in the system
S_n	Susceptible population without vaccination
S_v	Susceptible population with vaccination
D	Death population
R	Recovered population
Z	Final size
PCR	Primary course rate, two doses in total
BDR	Booster dose rate, three doses in total

Table 2
The PCR and BDR in Spain(COVID-19 Vaccine Tracker | European, 2022).

week	2021-W52	2022-W2	2022-W4	2022-W6	2022-W8	Mean
PCR	75%	75.3%	75.5%	76.2%	77%	75.8%
BDR	30.1%	37.4%	45%	48.8%	50.5%	42.36%

Table 3
The PCR and BDR in Norway(COVID-19 Vaccine Tracker | European, 2022).

week	2022-W2	2022-W4	2022-W6	2022-W8	2022-W10	2022-W12	Mean
PCR	73.7%	74.2%	74.6%	74.7%	74.8%	74.8%	74.47%
BDR	42.0%	49.9%	52.6%	53.5%	53.8%	54%	50.97%

1 Individuals with uptake booster dose have gotten primary course.
2 The mean PCR and BDR are used to calculate the vaccine effectiveness.

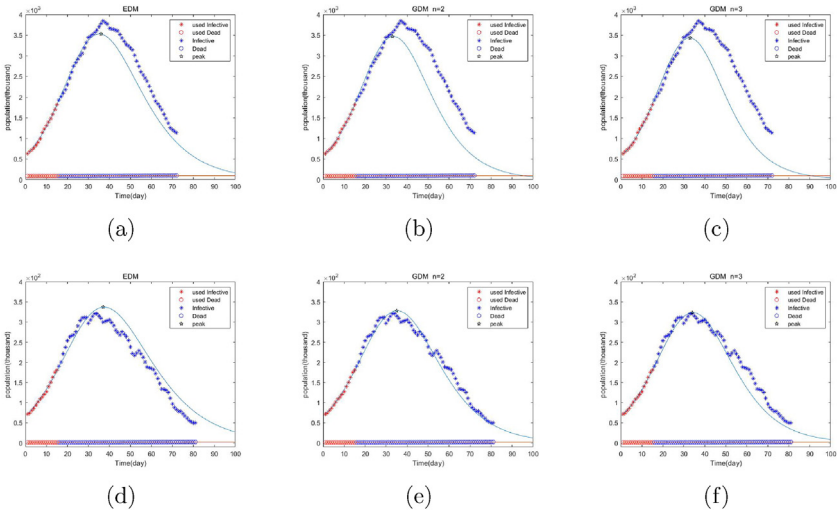

Fig. 6. (a), (b) and (c) show the fitting results of EDM, GDM ($n=2$), GDM ($n=3$) for Spanish data, respectively. (d), (e) and (f) show the fitting results of EDM, GDM ($n=2$), GDM ($n=3$) for Norwegian data, respectively. In the figure, the asterisk * represents the number of active infectious individuals per day and the circle ∘ represents cumulative deaths. Where the red markers are the data used for the fit and the blue are the data not used.

Table 4
Parameter values in Spain.

Parameters	Values	Unit	Definitions	Reference
β_1	$9.1376*10^{-9}$	$1/(individual \times day)$	Transmission coefficient of EDM	Fitting
β_2	$8.5194*10^{-9}$	$1/(individual \times day)$	Transmission coefficient of GDM ($n=2$)	Fitting
β_3	$8.3008*10^{-9}$	$1/(individual \times day)$	Transmission coefficient of GDM ($n=3$)	Fitting
ϵ	44.4%	dimensionless	Vaccine lose effectiveness	(33)
Γ	1/6.5	1/day	Recovery rate of infected individuals in EDM	Yuan et al. (2022)
γ_1	1/6.5	1/day	Recovery rate of infected individuals in GDM	Yuan et al. (2022)
S_{n0}	$1.0959*10^{7}$	persons	Initial number of S_n	(35)
S_{v0}	$3.4326*10^{7}$	persons	Initial number of S_v	(36)
I_0	$6.26678*10^{5}$	persons	Initial number of I	Fig. 5
D_0	$8.9019*10^{4}$	persons	Initial number of D	Fig. 5
P	0.03%	dimensionless	Infection fatality rate	Ulloa et al. (2022)

Table 5
Parameter values in Norway.

Parameters	Values	Unit	Definitions	Reference
β_1	$7.5348*10^{-8}$	$1/(individual \times day)$	Transmission coefficient of EDM	Fitting
β_2	$7.0752*10^{-8}$	$1/(individual \times day)$	Transmission coefficient of GDM ($n=2$)	Fitting
β_3	$6.9124*10^{-8}$	$1/(individual \times day)$	Transmission coefficient of GDM ($n=3$)	Fitting
ϵ	40%	dimensionless	Vaccine lose effectiveness	(34)
Γ	1/6.5	1/day	Recovery rate of infected individuals in EDM	Yuan et al. (2022)
γ_1	1/6.5	1/day	Recovery rate of infected individuals in GDM	Yuan et al. (2022)
S_{n0}	$4.0484*10^{6}$	persons	Initial number of S_n	(35)
S_{v0}	$1.3879*10^{6}$	persons	Initial number of S_v	(36)
I_0	$7.2318*10^{4}$	persons	Initial number of I	Fig. 5
D_0	$1.379*10^{3}$	persons	Initial number of D	Fig. 5
P	0.03%	dimensionless	Infection fatality rate	Ulloa et al. (2022)

Table 6
Comparison of the three model fitting results with the real data in Spain.

	Error	Peak value	Peak time	Final size
Real data	0	$3.846305*10^{6}$	2022/1/28	$5.382421*10^{6}$
EDM	6.10%	$3.530329*10^{6}$	2022/1/26	$2.4673966*10^{7}$
GDM ($n=2$)	11.86%	$3.469738*10^{6}$	2022/1/24	$2.2322434*10^{7}$
GDM ($n=3$)	14.32%	$3.435796*10^{6}$	2022/1/24	$2.1317022*10^{7}$

1 Final size is taken as the cumulative number of infected individuals from December 23, 2021 to March 4, 2022.
2 Error is given by Equation (37) from January 8 to March 4, 2022.

3.4. Effectiveness of different interventions on EDM and GDM

In this section, we will use EDM and GDM to evaluate the effectiveness of different interventions in this epidemic in Spain and Norway. We examine how the models may provide different evaluations on the effectiveness of different interventions. Three control strategies are proposed for Spain and Norway, respectively. Some of the main indicators used to assess the effectiveness of the control strategy include the final size, peak value and peak time of the outbreak. The simulation results are shown in Figs. 7–10.

Figs. 7 and 8 show the numerical simulations of EDM, GDM ($n=2$) and GDM ($n=3$) based on Spanish and Norwegian parameters. It plots active infectious individuals (thin solid curve), cumulative infections (thick solid curve) and cumulative deaths (dashed curve). The four rows compare for scenarios based on wearing masks to reduce transmission rates (β) and/or increasing the rate of vaccination(PCR, BDR). It includes one baseline scenario and three strategies. See Table 8 for details.

We observe from (7) and (8) that when the transmission coefficient (β) is reduced (Baseline scenario and Strategies I), all three models for two countries show reductions in final size and peak value as well as delayed peak time (see rows 1–2). All three models also show similar (Spain) or stronger (Norway) effects for Strategies I and II (see rows 2–3), which suggests that increasing the rate of vaccination and reducing the transmission coefficient have similar effects. Strategy III contains both Strategy I and Strategy II. Comparing Strategy I and Strategy II (see rows 2–4), we can see that the two measures work together (Strategy III) best.

Fig. 9 shows a more detailed comparison of the final size, peak value and time for the three control strategies in Spain and Norway. In particular, if we compare Strategy I, Strategy II and Strategy III, they all lead to smaller disease sizes, but Strategy III leads to a earlier peak time. More importantly, we find that the three models provide a consistent assessment of the control strategy. We also observe that EDM has larger final size, peak time and smaller peak value, while GDM, especially GDM ($n=3$)

Table 7
Comparison of the three model fitting results with the real data in Norway.

	Error	Peak value	Peak time	Final size
Real data	0	$3.21288*10^5$	2022/2/10	$9.67323*10^5$
EDM	11.52%	$3.37202*10^5$	2022/2/13	$2.637953*10^6$
GDM ($n=2$)	6.39%	$3.28280*10^5$	2022/2/11	$2.360852*10^6$
GDM ($n=3$)	9.54%	$3.23695*10^5$	2022/2/10	$2.244447*10^6$

1 Final size is taken as the cumulative number of infected individuals from January 8 to March 29, 2022.
2 Error is given by Equation (37) from January 23rd to March 29th, 2022.

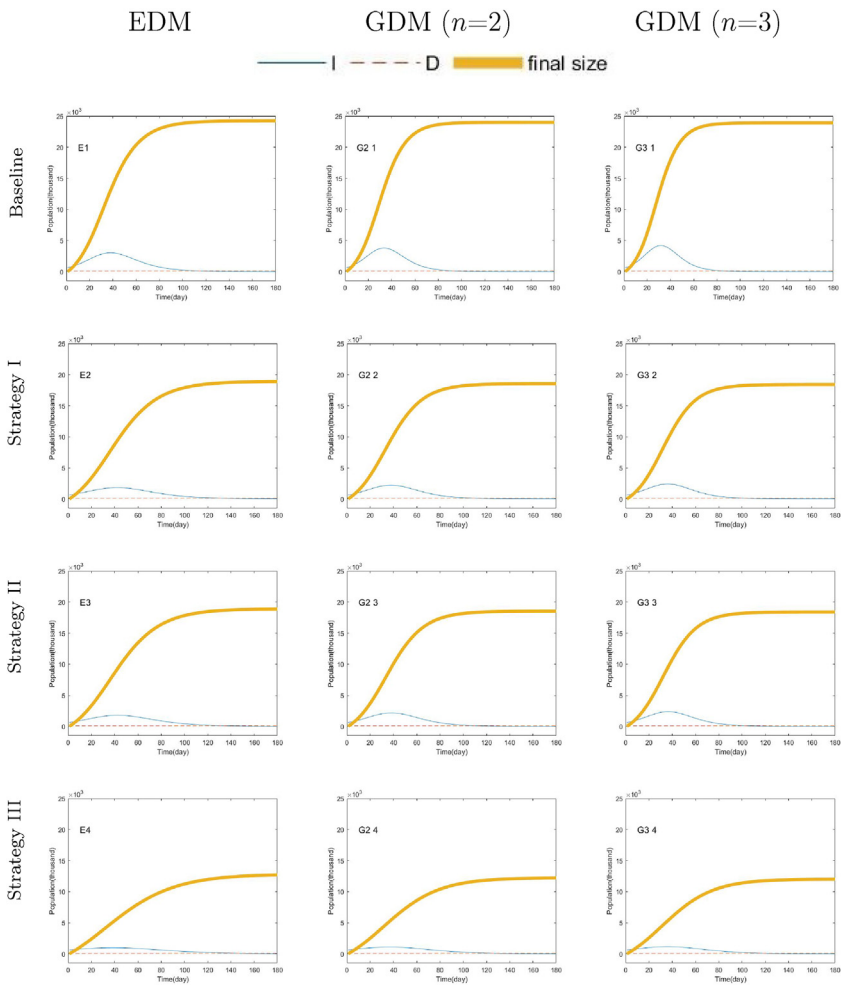

Fig. 7. Comparison of the epidemic sizes generated by the models EDM, GDM ($n=2$) and GDM ($n=3$) based on Spanish parameters for the baseline scenario (top row) and strategies I, II and III (rows 2, 3 and 4, respectively).

has smaller final size, peak time and larger peak value. Therefore, when we use a mathematical model to describe disease transmission, we will get an overestimation of the peak value and an underestimation of the final size and peak time, assuming the gamma distribution for the infectious period (the truth is an exponential distribution). In contrast, we will underestimate the peak value and overestimate the final size and peak time, assuming the exponential distribution for the infectious period (the truth is a gamma distribution).

From (22) and (32), it is clear that GDM and EDM have the same $\Re_0$ (because of $\gamma=\gamma_1$). Fig. 10 shows the contour plot (when β is fixed as Baseline scenario) of $\Re_0$ and the surface plot for $\Re_0=1$. Above the surface means $\Re_0<1$ (the disease will not break out), below the surface means the disease will break out. Panel (a) shows that disease outbreaks can be stopped by vaccination only, and panel (b) shows that vaccination can reduce the $\Re_0$ to below 1 more quickly if it is accompanied by a lower transmission coefficient.

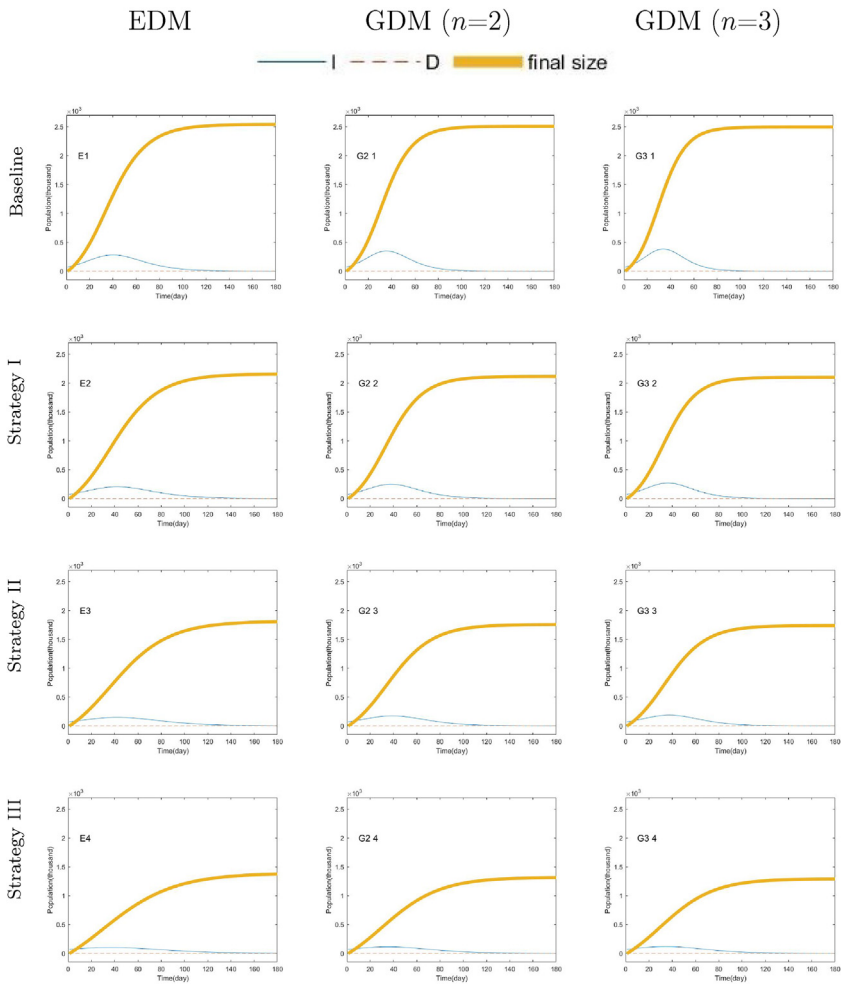

Fig. 8. Comparison of the epidemic sizes generated by the models EDM, GDM ($n = 2$) and GDM ($n = 3$) based on Norwegian parameters for the baseline scenario (top row) and strategies I, II and III (rows 2, 3 and 4, respectively).

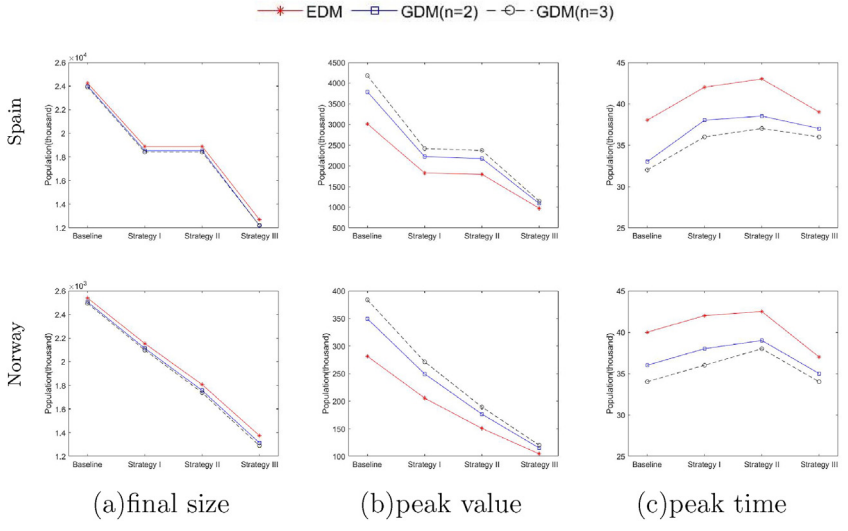

Fig. 9. Comparison of the final size (a), peak value (b) and peak time (c) generated by the three models under the baseline scenario and the three control strategies I, II and III, in Spain and Norway.

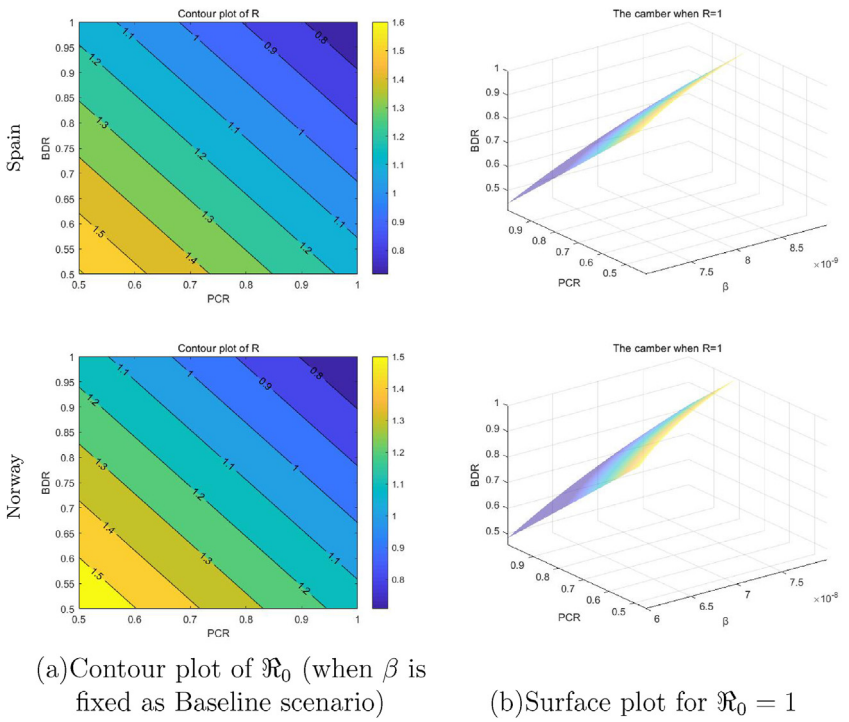

(a)Contour plot of $\Re_0$ (when β is fixed as Baseline scenario) (b)Surface plot for $\Re_0 = 1$

Fig. 10. Panel (a) shows the scenario of prevention and control only through vaccine without affecting people's normal travel life. Panel (b) includes vaccines and restrictions on life travel.

Table 8
Three control strategies in Spain and Norway.

	Spain	Norway
Baseline scenario	$\beta = 8.5*10^{-9}$ and PCR = 75.8%,BDR = 42.36%	$\beta = 7.0*10^{-8}$ and PCR = 74.47%,BDR = 50.97%
Strategy I	$\beta = 7.5*10^{-9}$ and PCR = 75.8%,BDR = 42.36%	$\beta = 6.5*10^{-8}$ and PCR = 74.47%,BDR = 50.97%
Strategy II	$\beta = 8.5*10^{-9}$ and PCR = 85.8%,BDR = 52.36%	$\beta = 7.0*10^{-8}$ and PCR = 84.47%,BDR = 60.97%
Strategy III	$\beta = 7.5*10^{-9}$ and PCR = 85.8%,BDR = 52.36%	$\beta = 6.5*10^{-8}$ and PCR = 84.47%,BDR = 60.97%

4. Conclusions

In the present paper, we propose and analyze two SIR epidemic models with exponential and gamma distribution for infectious period (EDM and GDM, respectively). Theoretically, we derive the analytic formulas for basic reproduction number, peak value, peak time as well as final size of EDM; For GDM, we obtain its basic reproduction number, maximum epidemic size value as well as its final size of GDM.

We perform the methods of least-squares fits to the EDM and GDM using data from the COVID-19 (Omicron) epidemic in Spain and Norway, respectively. From Tables 6 and 7 and Fig. 6, we find that the COVID-19 (Omicron) epidemic in Spain is more suitable for the EDM model, while the COVID-19 (Omicron) epidemic in Norway is more suitable for the GDM model. Therefore, we speculate that the same infectious disease has different distribution for the infectious period in different countries or regions, which also suggests that the assumption of distribution for the infectious period has significant effectiveness, when we use mathematical models to describe disease transmission, the assumptions for distribution of the infectious period must be carefully made.

Finally, we evaluate the effect of EDM and GDM on control strategies. Using the Spanish and Norwegian data as the basic parameters for the numerical simulations, we consider three different control strategies. The numerical simulation results show that the assessment of the three strategies by EDM and GDM is synchronous. However, EDM may result in larger final size, peak time and smaller peak value compared to GDM. Therefore, in infectious disease models, if we make unreasonable assumptions about the distribution for the infectious period, we may over- or underestimate peak value, final size and peak time.

The models in this paper are the simplest SIR models, and it remains open whether the more general (realistic) model would yield the same conclusions, which we leave as our future work.

Acknowledgements

The authors would like to thank Nannan Li (Tiangong University) and Shanshan Song (Tiangong University) for their valuable advice and insights provided for this paper.

This research was supported by the National Natural Science Foundation of China (12271401, 11871179, 11771128, 12171291), the Fund Program for the Scientific Activities of Selected Returned Overseas Professionals in Shanxi Province (20200001), and the Fundamental Research Program of Shanxi Province (202103021224018).

References

Andrews, N., Stowe, J., Kirsebom, F., et al. (2021). Effectiveness of COVID-19 vaccines against the Omicron (B.1.1.529) variant of concern. *medRxiv*. https://doi.org/10.1101/2021.12.14.21267615, 12.14.21267615.

An, R., Hu, J., & Wen, L. (2021). A nonlinear model predictive control model aimed at the epidemic spread with quarantine strategy. *Journal of Theoretical Biology, 531*, Article 110915. https://doi.org/10.1016/j.jtbi.2021.110915. ISSN 0022-5193.

Arino, J., Brauer, F., van den Driessche, P., Watmough, J., & Wu, J. (2007). A final size relation for epidemic, models. *Mathematical Biosciences and Engineering, 4*, 159–175.

Blyuss, K. B., & Kyrychko, Y. N. (2021). Effects of latency and age structure on the dynamics and containment of COVID-19. Mar 21 *Journal of Theoretical Biology, 513*, Article 110587. https://doi.org/10.1016/j.jtbi.2021.110587.

Bolzoni, L., Della Marca, R., & Groppi, M. (2021). On the optimal control of SIR model with Erlang-distributed infectious period: Isolation strategies. *Journal of Mathematical Biology, 83*, 36. https://doi.org/10.1007/s00285-021-01668-1

Braud, G. (2018). Mathematical models and vaccination strategies. *Vaccine, 36*, 5366–5372. https://doi.org/10.1016/j.vaccine.2017.10.014. ISSN 0264-410X.

Brauer, F. (2015). Some simple nosocomial disease transmission models. *Bulletin of Mathematical Biology, 77*, 460–469. https://doi.org/10.1007/s11538-015-0061-0

Capistran, M. A., Capella, A., & Christen, J. A. (2021). Forecasting hospital demand in metropolitan areas during the current COVID-19 pandemic and estimates of lockdown-induced 2nd waves. Jan 22 *PLoS One, 16*(1), Article e0245669. https://doi.org/10.1371/journal.pone.0245669.

Coronavirus COVID-19 (2019-nCoV) (arcgis.com) https://www.arcgis.com/apps/dashboards/bda7594740fd40299423467b48e9ecf6. (Accessed 20 August 2022).

COVID-19 Weekly cases and deaths per 100,000 population by age, race/ethnicity, and sex. https://covid.cdc.gov/covid-data-tracker/#demographicsovertime. (Accessed 20 August 2022).

COVID-19 Vaccine tracker | European centre for disease prevention and control (europa.eu). https://vaccinetracker.ecdc.europa.eu/public/extensions/COVID-19/vaccine-tracker.html#national-ref-tab. (Accessed 20 August 2022).

Djaoue, S., Kolaye, G. G., Abboubakar, H., Ari, A. A. A., & Damakoa, I. (2020). Mathematical modeling, analysis and numerical simulation of the COVID-19 transmission with mitigation of control strategies used in Cameroon, Chaos. *Solitons & Fractals, 139*, Article 110281. https://doi.org/10.1016/j.chaos.2020.110281. ISSN 0960-0779.

van den Driessche, P., & Watmough, J. (2008). Further notes on the basic reproduction number. In F. Brauer, P. van den Driessche, & J. Wu (Eds.), *Mathematical epidemiology. Lecture notes in mathematics, 1945*. Berlin, Heidelberg: Springer. https://doi.org/10.1007/978-3-540-78911-6_6.

Feng, Z. (2007). Final and peak epidemic sizes for SEIR models with quarantine and isolation. *Mathematical Biosciences and Engineering, 4*, 675–686.

Feng, Z., & Thieme, H. R. (2000). Endemic models with arbitrarily distributed periods of infection I: Fundamental properties of the model. *SIAM Journal on Applied Mathematics, 61*(3), Article 803C833.

Feng, Z., Xu, D., & Zhao, H. (2007). Epidemiological models with non-exponentially distributed disease stages and applications to disease control. *Bulletin of Mathematical Biology, 69*, 1511–1536.

Feng, Z., Zheng, Y., Hernandez-Ceron, N., Zhao, H., Glasser, J. W., & Hill, A. N. (2016). Mathematical models of Ebola-Consequences of underlying assumptions. *Mathematical Biosciences, 277*, 89–107. https://doi.org/10.1016/j.mbs.2016.04.002

Greenhalgh, D. (1992). Some results for an SEIR epidemic model with density dependence in the death rate. *IMA Journal of Maths with Applications in Medicine & Biology, 9*, 67–106. https://doi.org/10.1093/imammb/9.2.67

Humphrey, L., Thommes, E. W., Fields, R., Coudeville, L., Hakim, N., Chit, A., Wu, J., & Cojocaru, M. G. (2021). Large-scale frequent testing and tracing to supplement control of Covid-19 and vaccination rollout constrained by supply. *Infectious Disease Modelling, 6*, 955–974. https://doi.org/10.1016/j.idm.2021.06.008. ISSN 2468-0427.

Kabir, K. M. A., Risa, T., & Tanimoto, J. (2021). Prosocial behavior of wearing a mask during an epidemic: An evolutionary explanation. *Scientific Reports, 11*, Article 12621. https://doi.org/10.1038/s41598-021-92094-2

Kermack, W. O., & McKendrick, A. G. (1927). A contribution to the mathematical theory of epidemics. *Proceedings of. Royal Society Londdon.A, 115*, Article 700C721.

O. Krylova, D. J. D. Earn, Effects of the infectious period distribution on predicted transitions in childhood disease dynamics, Journal of The Royal Society Interface 10:20130098. doi: http://doi.org/10.1098/rsif.2013.0098.

Kuznetsov, Y. A., & Piccardi, C. (1994). Bifurcation analysis of periodic SEIR and SIR epidemic models. *Journal of Mathematical Biology, 32*, 109–121. https://doi.org/10.1007/BF00163027

Li, M. Y., & Muldowney, J. S. (1995). Global stability for the SEIR model in epidemiology. *Mathematical Biosciences, 125*, 155–164. https://doi.org/10.1016/0025-5564(95)92756-5

Li, Q., Tang, B., Bragazzi, N. L., Xiao, Y., & Wu, J. (2020). Modeling the impact of mass influenza vaccination and public health interventions on COVID-19 epidemics with limited detection capability. *Mathematical Biosciences, 325*, Article 108378. https://doi.org/10.1016/j.mbs.2020.108378. ISSN 0025-5564.

Liu, X., Takeuchi, Y., & Iwami, S. (2008). SVIR epidemic models with vaccination strategies. *Journal of Theoretical Biology, 253*, 1–11. https://doi.org/10.1016/j.jtbi.2007.10.014. ISSN 0022-5193.

A. L. Lloyd, Destabilization of epidemic models with the inclusion of realistic distributions of infectious periods, Proceedings of Royal Soceity B 268(1470): 985-993. doi: http://doi.org/10.1098/rspb.2001.1599.

Ma, J., & Earn, D. J. D. (2006). Generality of the final size formula for an epidemic of a newly invading infectious disease. *Bulletin of Mathematical Biology, 68*, 679–702. https://doi.org/10.1007/s11538-005-9047-7

Musa, S. S., Qureshi, S., Zhao, S., Yusuf, A., Mustapha, U., & He, D. (2021). Mathematical modeling of COVID-19 epidemic with effect of awareness programs. *Infectious Disease Modelling, 6*, 448–460. https://doi.org/10.1016/j.idm.2021.01.012. ISSN 2468-0427.

Norway Population. (2022). Worldometer (worldometers.info). https://www.worldometers.info/world-population/norway-population/. (Accessed 20 October 2022).

Norway COVID - coronavirus statistics - worldometer (worldometers.info). https://www.worldometers.info/coronavirus/country/norway/. (Accessed 20 August 2022).

Norway Age structure - Demographics (indexmundi.com). https://www.indexmundi.com/norway/age_structure.html. (Accessed 20 August 2022).

Okuonghae, D. (2013). A mathematical model of tuberculosis transmission with heterogeneity in disease susceptibility and progression under a treatment regime for infectious cases. *Applied Mathematical Modelling, 37*, 6786–6808. https://doi.org/10.1016/j.apm.2013.01.039. ISSN 0307-904X.

Ontario population projections. https://www.ontario.ca/page/ontario-population-projections. (Accessed 20 August 2022).

N. A Sivadas, A. Mahajan, P. Panda, Control Strategies for the Third wave of COVID-19 infection in India: A Mathematical Model Incorporating Vaccine Effectiveness, TechRxiv. Preprint. doi: https://doi.org/10.36227/techrxiv.17705957.v1.

Song, H., Fan, G., Zhao, S., Li, H., Huang, Q., & He, D. (2021b). Forecast of the COVID-19 trend in India: A simple modelling approach. *Mathematical Biosciences and Engineering, 18*, 9775–9786. https://doi.org/10.3934/mbe.2021479

Song, H., Jia, Z., Jin, Z., & Liu, S. (2021a). Estimation of COVID-19 outbreak size in Harbin, China. *Nonlinear Dynamics, 106*, 1229–1237. https://doi.org/10.1007/s11071-021-06406-2

Song, H., Li, F., Jia, Z., Jin, Z., & Liu, S. (2020). Using traveller-derived cases in Henan Province to quantify the spread of COVID-19 in Wuhan, China. *Nonlinear Dynamics, 101*, 1821–1831. https://doi.org/10.1007/s11071-020-05859-1

Song, H., Liu, F., Li, F., Cao, X., Wang, H., Jia, Z., Zhu, H., Li, M. Y., Lin, W., Yang, H., Hu, J., & Jin, Z. (2022). Modeling the second outbreak of COVID-19 with isolation and contact tracing. *Discrete and Continuous Dynamical Systems - Series B, 27*, 5757–5777. https://doi.org/10.3934/dcdsb.2021294

Spain Population. (2022). Worldometer (worldometers.info). https://www.worldometers.info/world-population/spain-population/. (Accessed 20 October 2022).

Spain COVID - coronavirus statistics - worldometer (worldometers.info). https://www.worldometers.info/coronavirus/country/spain/. (Accessed 20 August 2022).

Spain Age structure - Demographics (indexmundi.com). https://www.indexmundi.com/spain/age_structure.html. (Accessed 20 August 2022).

Starke, K. R., Petereit-Haack, G., Schubert, M., mpf, D. K., Schliebner, A., Hegewald, J., & Seidler, A. (2020). The age-related risk of severe outcomes due to COVID-19 infection: A rapid review, meta-analysis, and meta-regression. Aug 17 *International Journal of Environmental Research and Public Health, 17*(16), 5974. https://doi.org/10.3390/ijerph17165974.

Tomchin, D. A., & Fradkov, A. L. (2020). Prediction of the COVID-19 spread in Russia based on SIR and SEIR models of epidemics. *IFAC-PapersOnLine, 53*, 833–838.

Turkyilmazoglu, M. (2021). Explicit formulae for the peak time of an epidemic from the SIR model. *Physica D: Nonlinear Phenomena, 422*, Article 132902. https://doi.org/10.1016/j.physd.2021.132902. ISSN 0167-2789.

Ulloa, A. C., Buchan, S. A., Daneman, N., & Brown, K. A. (2022). Estimates of SARS-CoV-2 Omicron variant severity in Ontario, Canada. *JAMA, 327*, 1286–1288. https://doi.org/10.1001/jama.2022.2274

R. Verity et al., Estimates of the severity of coronavirus disease 2019: a model-based analysis. The Lancet Infectious Diseases 6, 669C677. doi: https://doi.org/10.1016/S1473-3099(20)30243-7.

Wang, X., Shi, Y., Feng, Z., & Cui, J. (2017). Evaluations of interventions using mathematical models with exponential and non-exponential distributions for disease stages: The case of Ebola. *Bulletin of Mathematical Biology, 79*, 2149–2173. https://doi.org/10.1007/s11538-017-0324-z

Wearing, H. J., Rohani, P., & Keeling, M. J. (2005). Appropriate models for the management of infectious diseases. *PLoS Medicine, 2*, 621–627.

Wei, H., Musa, S. S., Zhao, Y., & He, D. (2022). Modelling of waning of immunity and reinfection induced antibody boosting of SARS-CoV-2 in Manaus, Brazil. *International Journal of Environmental Research and Public Health, 19*, 1729. https://doi.org/10.3390/ijerph19031729

Yuan, P., Aruffo, E., Tan, Y., Yang, L., Ogden, N. H., Fazil, A., & Zhu, H. (2022). Projections of the transmission of the Omicron variant for Toronto, Ontario, and Canada using surveillance data following recent changes in testing policies. *Infectious Disease Modelling, 7*, 83–93. https://doi.org/10.1016/j.idm.2022.03.004